Published in final edited form as:
Mutat Res. 2012 July 1; 735(1-2): 39–45. doi:10.1016/j.mrfmmm.2012.04.004.

Prdx1 deficiency in mice promotes tissue specific loss of heterozygosity mediated by deficiency in DNA repair and increased oxidative stress

Vamsi Rani[1], **Carola A. Neumann**[2], **Changshun Shao**[1], and **Jay A. Tischfield**[1]

[1]Department of Genetics and the Human Genetics Institute of New Jersey, Rutgers University, 145 Bevier Road, Piscataway, NJ 08854 USA

[2]Department of Cell and Molecular Pharmacology and Experimental Therapeutics, Medical University of South Carolina, 173 Ashley Ave MSC-505, Charleston, SC 29425 USA

Abstract

The loss of the H_2O_2 scavenger protein encoded by Prdx1 in mice leads to an elevation of reactive oxygen species (ROS) and tumorigenesis of different tissues. Loss of heterozygosity (LOH) mutations could initiate tumorigenesis through loss of tumor suppressor gene function in heterozygous somatic cells. A connection between the severity of ROS and the frequency of LOH mutations *in vivo* has not been established. Therefore, in this study, we characterized *in vivo* LOH in ear fibroblasts and splenic T cells of 3–4 month old Prdx1 deficient mice. We found that the loss of Prdx1 significantly elevates ROS amounts in T cells and fibroblasts. The basal amounts of ROS were higher in fibroblasts than in T cells, probably due to a less robust Prdx1 peroxidase activity in the former. Using *Aprt* as a LOH reporter, we observed an elevation in LOH mutation frequency in fibroblasts, but not in T cells, of *Prdx1*$^{-/-}$ mice compared to *Prdx1*$^{+/+}$ mice. The majority of the LOH mutations in both cell types were derived from mitotic recombination (MR) events. Interestingly, *Mlh1*, which is known to suppress MR between divergent sequences, was found to be significantly down-regulated in fibroblasts of *Prdx1*$^{-/-}$ mice. Therefore, the combination of elevated ROS amounts and down-regulation of *Mlh1* may have contributed to the elevation of MR in fibroblasts of *Prdx1*$^{-/-}$ mice. We conclude that each tissue may have a distinct mechanism through which Prdx1 deficiency promotes tumorigenesis.

Keywords

reactive oxygen species; loss of heterozygosity; peroxiredoxin 1; mutations

1. Introduction

Reactive oxygen species (ROS), specifically, superoxide radicals (O_2^-), are produced as the by-products of mitochondrial oxidative phosphorylation and various metabolic processes.

Corresponding author: Jay Tischfield, Tel: 732-445-1027, jay@biology.rutgers.edu.

Conflict of Interest
The authors declare no conflict of interest.

The superoxide radicals are dismutated to hydrogen peroxide (H_2O_2) by a family of superoxide dismutase (Sod) enzymes functional in different sub-cellular compartments [1]. H_2O_2 is then converted to H_2O and O_2 by different families of peroxidases: catalase, glutathione peroxidases (Gpxs) and peroxiredoxins (Prdxs). Prdx1 is easily over-oxidized due to its Cys^{51} that during catalysis exists as thiolate anion, whereas the other cysteines (Cys^{17}, Cys^{80} and Cys^{172}) remain protonated at neutral pH. The thiolate Cys^{51} is very unstable and highly reactive with any accessible thiol to form either a disulfide or to further oxidize to sulfinic or sulfonic acid structures [2], which are believed to possess peroxidase-inactive chaperone functions (reviewed in [3]). The switch to chaperone functionality leads to catalase activity that scavenges more of the cellular H_2O_2. Overall, the peroxidases sequentially maintain homeostatic amounts of H_2O_2, which curtails the formation of highly reactive hydroxyl (OH•) radicals (through the Fenton reaction).

Elevated amounts of intracellular ROS (oxidative stress) produced as a result of an exogenous stressor (e.g., H_2O_2 or irradiation) can damage DNA, protein and lipids through oxidation. At least 100 different types of oxidative DNA lesions are known to form, which include base modifications (e.g. 8-oxo-guanine (8-oxoG), thymidine glycol & 8-hydroxycytosine), single-strand breaks (SSBs), double-strand breaks (DSBs) and interstrand cross-links [4]. For example, H_2O_2 treatment of human T-lymphocytes led to increased *Hprt* mutant frequency with a majority of mutations classified as transitions at GC base pairs [5]. Additionally, oxidative DNA damage could stem from compromised ROS scavenging such as in the case of Prdx1 deficient mouse embryonic fibroblasts (MEFs) that exhibited increased ROS amounts compared to wild-type MEFs and an elevated number of 8-oxoG DNA lesions [6]. Moreover, there was also greater oxidation of hemoglobin in Prdx1 deficient erythrocytes as evidenced by the appearance of Heinz bodies and eventual hemolytic anemia. A separate study involving adult *Prdx1*$^{-/-}$ mice found increased levels of various types of oxidative DNA lesions in the brain, spleen and liver [7]. In addition to causing DNA base damage, elevated ROS could also lead to increased frequency of loss of heterozygosity (LOH) mutations primarily derived from mitotic recombination (MR) events that originated in response to the need for DNA DSB repair [8, 9].

LOH is frequently a rate-limiting step in tumorigenesis [10] and increased frequency of LOH mutations is positively correlated with increased cancer incidence such as that which is observed in Prdx1-deficient mice [6]. We have previously utilized *Aprt*$^{+/-}$ mice as a model system to study *in vivo* LOH [11, 12]. Cells that have undergone *in vivo* LOH that includes *Aprt* are recovered as cell colonies *in vitro* by virtue of their resistance to 2,6-diaminopurine (DAP). The recovered colonies can then be analyzed to determine the mutational mechanism that produced the *in vivo* LOH. In order to determine whether LOH is elevated *in vivo* by ROS, which may consequently contribute to increased tumorigenesis, we measured the spontaneous LOH mutant frequencies in ear fibroblasts and splenic T cells of Prdx1 deficient mice. We observed that while ROS amounts are increased in both fibroblasts and T cells derived from *Prdx1*$^{-/-}$ mice, they are much higher in fibroblasts than in T cells regardless of *Prdx1* functional status. Correspondingly, significant elevations in *Aprt* LOH mutant frequencies were found only in *Prdx1*$^{+/-}$ and *Prdx1*$^{-/-}$ fibroblasts.

2. Materials and Methods

2.1 Mice Breeding

129XC57 *Prdx1*$^{+/-}$ and *Prdx1*$^{-/-}$ male mixed strain mice were as described [6]. These mice were backcrossed to 129 strain and C57 strain, respectively, for four generations. We utilized “speed congenics” by analyzing distribution of microsatellite markers along chromosome 8 to determine the appropriate mice for mating for the subsequent generation until pure strain 129 or C57 mice were generated. The N4 129 *Prdx1*$^{+/-}$ mice were then

crossed with 129 *Aprt*$^{+/-}$ mice to generate N5 129 *Prdx1*$^{+/-}$ *Aprt*$^{+/-}$ mice. These mice were then crossed with N4 C57 *Prdx1*$^{+/-}$ mice to generate N5 129X N4 C57 hybrid *Prdx1* (+/+, +/− and −/−) *Aprt*$^{+/-}$ mice.

2.2 Cell culture and calculations of Aprt mutant frequency

Ear fibroblasts and splenic T cells were derived from 3–4 month old mice as described in previous studies [11,13,14]. We recovered DAP-resistant (DAP^r) clones from fibroblasts (100mm plates) and T cells (96-well plates) by culturing them in supplemented DMEM or RPMI medium (Hyclone), respectively, containing 50μg/ml DAP. DAP^r colonies were picked at day 12 or day 9 after plating, for fibroblasts and T cells, respectively. At the same time, plates for colony-forming efficiency were established for fibroblasts (1×10^4 cells/plate) and T cells (4 cells/well) and positive colonies counted at day 11 or day 8 after plating, respectively. Colony-forming efficiency and DAP^r mutant frequency calculations were done as previously described [13].

2.3 Molecular Analyses of DAP^r clones

DAP^r mutant clones were classified into class I or class II by loss or presence of the *Aprt*$^+$ allele, as described elsewhere (11). Class I clones were further characterized using microsatellite markers along chromosome 8 (*D8Mit56, 271, 106, 125* and *155*). Clones that exhibited LOH at distal loci, including *Aprt*, but remained heterozygous near the centromere were considered to be derived from mitotic recombination (MR). Class I clones with LOH at both *D8Mit56* (telomeric) and *D8Mit155* (centromeric) were regarded as the product of chromosomal loss (CL), and clones that did not exhibit LOH at *D8Mit56* and *D8Mit155* were classified as originating from either gene conversion (GC) or interstitial deletion (ID).

2.4 ROS measurements

Prior to plating the cells for the *Aprt* LOH studies, 1×10^5 concanavalin A (ConA) splenic T cells and ear fibroblasts were incubated with 5μM of 5-(and-6)-chloromethyl-2',7'-dichlorodihydrofluorescein diacetate (CM-H2DCFDA, Invitrogen™) (DCF) in the dark at 37°C for 22 minutes. Background controls included cells in medium without DCF. The cells were centrifuged, resuspended in 1X PBS, for flow cytometry analyses using the Beckman Coulter FC500 Analyzer with 10,000 cells gated for each cell type, and fluorescence (Excitation: 488nm, Emission: 525nm) measured using the FL1 channel.

2.5 RNA extraction and gene expression studies

RNA was isolated from 1×10^6 primary ear fibroblasts and 1×10^6 ConA stimulated T cells from 3–4 month old *Prdx1*$^{+/+}$ and *Prdx1*$^{-/-}$ mice (n=3) using the Qiagen RNeasy Mini Kit using the recommended protocol with the optional DNase on-column treatment. Concentration of RNA, 260/280 and 260/230 values were measured using the ND-1000 spectrophotometer with integrity of RNA (18s and 28s bands) determined through agarose gel electrophoresis. Each RNA sample was reverse transcribed to cDNA using the TaqMan® Reverse Transcription Reagents (Applied Biosystems™). RNA expression of the genes in Table 1 was measured using the Applied Biosystems 7900HT Sequence Detection System with B-actin as the loading control. PCR conditions were: 50°C for 2 minutes, 95°C for 10 min followed by 40 cycles of 95°C for 15s and 60°C for 1 min. The primer sequences were designed using the Primer Express v2.0 software and each sample-primer pair was run in triplicate.

2.6 Prdx1 western blot analyses

Primary ear fibroblasts and ConA stimulated T cells from 3–4 month old *Prdx1*$^{+/+}$ mice were isolated and cultured as described in the RNA expression studies. For this study, 1×10^6

T cells and 1×10^6 ear fibroblasts suspended in 1mL of their respective medium were used for each treatment group. Different concentrations of H_2O_2 (0, 20μM, 50μM and 250μM) were added directly to each cell suspension and incubated for 15 minutes in a 37°C, 95% RH and 10% CO_2 incubator. The suspension was then centrifuged, the pellet washed with PBS and the washed pellet resuspended in 150μL of protein extraction buffer (20mM HEPES and 0.1% Triton X-100, pH 7.4). The pellet was then centrifuged at 4000×g and the supernatant collected; protein concentration of the supernatant was determined by a standard BCA assay. 30μg of protein was analyzed for Prdx1 and Prdx1C53SO_3 protein expression under non-reducing and reducing (beta-mercaptoethanol added to extraction buffer) conditions. Actin was used as a loading control. All antibodies were from Abcam.

2.7 Statistical Analyses

The *Mann* Whitney U-test ($p<0.05$) was utilized to determine significant differences between median *Aprt* LOH mutant frequencies. Student t-test analysis was utilized to determine significance for DCF fluorescence measurements, with $p<0.05$ considered significant. For the gene expression analyses, a significant change was considered to be ≥ 2-fold difference with $p<0.05$ as determined by the student t-test.

3. Results

3.1 Increased ROS amounts in ear fibroblasts and splenic T cells of Prdx1$^{-/-}$ mice

We previously showed that loss of Prdx1 in MEFs led to increased amounts of ROS [6]; therefore, we wanted to determine if it had a similar impact in splenic T cells and in ear fibroblasts. ROS amounts were quantified by measuring the amount of intracellular CMH_2DCFDA that is cleaved by intracellular esterases and made fluorescent under oxidizing conditions [15]. Indeed, significantly higher amounts of ROS were observed with the complete loss of Prdx1 in both T cells and fibroblasts; ROS amounts were unaffected in *Prdx1*$^{+/-}$ T cells and *Prdx1*$^{+/-}$ fibroblasts (Figure 1A). Furthermore, the ROS amounts in fibroblasts, in general, were higher than in splenic T cells. To determine if this was due to differences in Prdx1 peroxidase activity between cell types, we examined Prdx1 protein monomer, dimer and oligomer formation in T cells and primary fibroblasts of *Prdx1*$^{+/+}$ mice after treatment with increasing concentrations of H_2O_2. The reduction of H_2O_2 to H_2O and O_2 by Prdx1 requires the formation of a disulfide bridge between two monomers, resulting in a dimer. In fibroblasts, with increasing concentrations of H_2O_2, we found a gradual decrease in dimer formation with a corresponding increase in monomer formation (Figure 1B-top panel), which was not observed in T cells except at the highest H_2O_2 treatment concentration (250μM) (Figure 1C-top panel). Moreover, we observed reducible Prdx1 oligomers only in the fibroblasts, which decreased after H_2O_2 treatment, suggesting greater H_2O_2-induced overoxidation of Prdx1 in those cells compared to T cells. Along those lines, an antibody specifically detecting Prdx1 overoxidized at its catalytic cysteine revealed a greater amount of overoxidized Prdx1 in fibroblasts compared to T cells (Figures 1B and 1C-bottom panels).

3.2 Increased LOH mutant frequency in ear fibroblasts of Prdx1$^{-/-}$ mice

Given the significant increase in ROS amounts observed in *Prdx1*$^{-/-}$ fibroblasts, we wanted to determine whether or not there was also a significant elevation of *in vivo* LOH mutant frequency as reported for *in vitro* LOH studies [8, 9]. There was a significant elevation (4.5-fold; $p=0.01$) in *Aprt* LOH mutant frequency in fibroblasts of *Prdx1*$^{-/-}$ mice compared to those of *Prdx1*$^{+/+}$ mice (Figure 2A and Table 2-top panel). Surprisingly, the *Prdx1*$^{+/-}$ fibroblasts in which ROS amounts were not detectably increased also had a significant elevation (2.3-fold; $p=0.04$) in *Aprt* LOH mutant frequency; however, no LOH was observed at the *Prdx1* locus in the *Prdx1*$^{+/-}$ clones (data not shown). The majority of *Aprt*

LOH clones across all *Prdx1* genotypes were designated as class I because they exhibited physical loss of the wild-type *Aprt* allele (Table 2-top panel). Consistent with *Aprt* LOH spectrums in previous reports, class I clones were derived primarily from MR as determined by chromosome 8 microsatellite marker analyses (Table 3). A small number of class I clones were derived from individual interstitial deletion/gene conversion (ID-GC) events in $Prdx1^{+/-}$ (4 clones) and $Prdx1^{-/-}$ (2 clones) fibroblasts, where each clone was independently derived from a different mouse. Additionally, six clones from one ear of a $Prdx1^{-/-}$ mouse exhibited LOH at all the marker loci tested (Table 3), suggesting that they may have been derived from chromosomal loss (CL). Because they were derived from a single mouse ear, they were probably sib clones.

3.3 LOH mutant frequency in T cells unaffected with loss of Prdx1

Unlike fibroblasts, no change in *Aprt* mutant frequency was observed in T cells with the loss of Prdx1 (Figure 2B and Table 2-bottom panel), although there was a significant elevation in the amounts of ROS (Figure 1A). All three Prdx1 genotypes exhibited a similar distribution of class I and class II *Aprt* LOH clones, with a slight but insignificant increase in the frequency of class I clones from $Prdx1^{-/-}$ mice (<2-fold) compared to $Prdx1^{+/+}$ mice (Table 2-bottom panel). The majority of *Aprt* LOH class I clones were derived from MR events (85% in $Prdx1^{+/+}$, 89% in $Prdx1^{+/-}$ and 91% in $Prdx1^{-/-}$) (Table 3). ID and GC events were responsible for the remaining $Prdx1^{+/+}$ (4 clones) and $Prdx1^{+/-}$ (3 clones) class I *Aprt* LOH clones, each derived from a different spleen. One $Prdx1^{-/-}$ class I *Aprt* LOH clone was derived from an ID-GC event and two clones exhibited LOH at all marker loci along the length of chromosome 8 (Table 3). Again, the two clones displaying whole chromosome LOH were derived from the same spleen and therefore, are considered sib clones.

3.4 Expression of antioxidant and DNA repair genes in $Prdx1^{-/-}$ cells

A previous study reported that elevated ROS amounts observed in phosphatase and tensin homolog (Pten) deficient MEFs was due to down-regulation in mRNA expression of various genes that encode antioxidant proteins (Prdx1, Prdx2, Prdx5, Prdx6 and Sod1) [16]. Additionally, the Prdx1 protein binds to and protects the Pten protein from oxidation-induced inactivation, thus acting as a safeguard of Pten [17]. Therefore, we hypothesized that the loss of Prdx1 could lead to greater Pten inactivation in $Prdx1^{-/-}$ T cells and ear fibroblasts, which would result in transcriptional down-regulation in expression of certain antioxidant proteins [16] contributing to the elevated ROS amounts observed in those cells (Figure 1A). In addition to the genes that are regulated by Pten, we also examined the transcriptional expression of other important H_2O_2 scavengers, catalase and Gpx1. In both T cells and fibroblasts, the loss of Prdx1 did not lead to significant differences in transcription of genes that encode antioxidant proteins (Figure 3). Therefore, the increased ROS amounts observed in $Prdx1^{-/-}$ T cells and fibroblasts seems entirely due to loss of Prdx1 antioxidant functionality and independent of changes in the activity of Pten.

Rad51 is a key component of DSB repair by homologous recombination. Since Pten positively regulates *Rad51* expression [18]; increased inactivation of Pten with the loss of Prdx1 could lead to decreased expression of Rad51 and decreased DSB repair. The mismatch repair gene, *Mlh1*, is also known to effect HR mediated DSB repair by preventing recombination between divergent sequences. We have previously shown that Mlh1 deficiency led to significant elevation of mitotic recombination (MR) in ear fibroblasts [12]. Therefore, changes in transcription of either of these genes could likely have an effect on the frequency of MR mediated LOH mutant frequency. In both T cells and fibroblasts, the loss of Prdx1 had no significant effect on *Rad51* expression. However, we found a significant 2-fold reduction in *Mlh1* expression in $Prdx1^{-/-}$ fibroblasts and a slightly less reduction in

Prdx1$^{-/-}$ T cells (1.7-fold) (Figure 4). The decrease in *Mlh1* expression could contribute to the increased frequency of LOH mutants in *Prdx1*$^{-/-}$ fibroblasts.

4. Discussion

We showed that the elevated ROS amounts in *Prdx1*$^{-/-}$ fibroblasts directly correlated to increased LOH mutant frequency, which we speculate is a direct consequence of an increased need for repair of DSBs through an increased accumulation of highly reactive OH• radicals [4] that occurs with the loss of Prdx1 [7]. Repair of DSBs could happen either by homologous recombination (HR) or non-homologous end-joining (NHEJ). A previous study found that mammalian cells in S-phase compared to cells in G1 phase are considerably more sensitive to the formation of DSBs induced by treatment with H_2O_2 [19]. It was hypothesized that the more open chromatin structure in S-phase makes DNA less protected against the attack by OH• radicals. This suggests that the repair of DSBs would rely more on HR than on NHEJ as NHEJ repair occurs primarily during the G1 phase. This could explain why the majority of the LOH mutants observed in *Prdx1*$^{-/-}$ fibroblasts were derived as a consequence of MR, a type of HR. Repair by NHEJ, which may result in deletion of several nucleotides around the DSB site, could be responsible for the interstitial deletion-gene conversion (ID-GC) events that took place in a small number of fibroblast clones.

Repair of DSBs by HR could be affected by deficiencies in other DNA repair pathways. The two-fold decrease in levels of *Mlh1* mRNA expression, a key mismatch repair (MMR) gene, in *Prdx1*$^{-/-}$ fibroblasts is significant because MMR is known to suppress recombination between divergent DNA sequences, presumably to minimize inappropriate genome rearrangements as a consequence of DNA DSB repair [12, 20]. MMR stalls strand exchange during HR in the presence of mismatches, resulting in stabilized branch intermediates [21]. The down-regulation of *Mlh1* in *Prdx1*$^{-/-}$ mice probably does not have a significant effect on MMR activity in T cells and its effect on the frequency of LOH mutations. Our previous study [12] found that while Mlh1 deficiency led to increased mitotic recombination (MR) in fibroblasts, it had no effect on MR in T cells. Instead, lack of Mlh1 led to increased point mutations, which was not observed in *Prdx1*$^{-/-}$ mice (data not shown). Because point mutations were not increased in Prdx1 deficient T cells (Table 3), the down-regulation of *Mlh1* apparently had no effect on MMR. The transcriptional down-regulation of *Mlh1* could be a consequence of increased methylation of the *Mlh1* promoter [22, 23] mediated by c-Myc deregulation and activation [24, 25], which is known to occur with the loss of Prdx1 [7]. Activation of c-Myc also led to increased formation of DSBs in rat fibroblasts, due to loss of checkpoint response during G1/S, and consequently premature passage through G1 [26]. This would allow DNA DSB breaks to accumulate during S-phase, which would require repair by recombination that conserves DNA sequence.

Although increased *Aprt* LOH frequency was detected in the ear fibroblasts of *Prdx1*$^{+/-}$ mice, it was not accompanied by increased intracellular amounts of ROS (Figure 1A). Thus, an increase in the amounts of ROS may not fully account for the increased LOH in fibroblasts of *Prdx1*$^{+/-}$ and *Prdx1*$^{-/-}$ mice. It has been previously reported that *Prdx1*$^{+/-}$ MEFs had significantly increased Ras mediated transformation in comparison to *Prdx1*$^{+/+}$ MEFs [7]. Therefore, we may speculate that increased c-Myc activation in *Prdx1*$^{+/-}$ fibroblasts lead to a compromise in G1/S checkpoint response, which in turn produced more DSBs. In *Prdx1*$^{-/-}$ fibroblasts, the increased activation of c-Myc may act synergistically with increased ROS amounts to promote LOH mutations that are mediated by HR. Another possibility is that cellular compartmentalization of limited amounts of the Prdx1 protein in *Prdx1*$^{+/-}$ fibroblasts may produce functional Prdx1 insufficiency in the nucleus relative to other cellular compartments. Thus, ROS levels could be increased in the nucleus but would be lower elsewhere in the cell, producing the observed average value for the entire cell.

Unlike our observations in *Prdx1*$^{-/-}$ fibroblasts, there was no correlation between elevated amounts of ROS and increased MR-mediated LOH mutant frequency in *Prdx1*$^{-/-}$ T cells. This disparity could be attributed to the much lower amounts of ROS in *Prdx1*$^{-/-}$ T cells relative to *Prdx1*$^{-/-}$ fibroblasts; ~4-fold lower ROS amounts were observed in *Prdx1*$^{+/+}$ T cells relative to *Prdx1*$^{+/+}$ fibroblasts (Figure 1A). Fibroblasts have reduced Prdx1 activity when compared to T cells, as evidenced by the greater formation of Prdx1 oligomers, monomers and the reduced formation of Prdx1 dimers compared to T cells when both are exposed to increasing amounts of H_2O_2 (Figures 1B and 1C). It has been shown that the extent of Prdx1 dimer formation is directly correlated to its catalytic activity because the Prdx1 catalytic cycle involves the formation of a disulfide bridge between the oxidized NH_2-terminal Cys^{51}-SOH on one monomer with the COOH-terminal Cys^{172}-SH on the other monomer, resulting in dimer formation [27]. The cycle is completed with the reduction of the cysteines to –SH by thioredoxin (Trx) [28]. However, Cys^{51}-SOH could be further oxidized to Cys^{51}-SO_2H before the formation of the disulfide bridge between Cys^{51} and Cys^{172}; the over-oxidized Cys^{51} cannot bond with Cys^{172}-SH [29] and thus results in inactivation of Prdx1 activity. In order to minimize this inactivation, cells have a sulfiredoxin protein that reduces Cys^{51}-SO_2H to Cys^{51}-SOH [27]. Therefore, sulfiredoxin activity could be lower in fibroblasts compared to T cells, leading to a greater overoxidation of Prdx1 in fibroblasts compared to T cells. Another possibility is decreased thioredoxin (Trx) enzyme activity in T cells compared to fibroblasts. Recently it has been described that the extent of H_2O_2-induced overoxidation of the Prdx catalytic cysteine is directly correlated with thioredoxin activity. It is therefore likely that over-oxidation of the catalytic Prdx cysteine occurs during catalysis by binding of Trx to Prdx-disulfides, where the reduction process renders the reduced Cys^{51}-SH to de-stabilization and over-oxidation in the presence of H_2O_2, by inhibiting the “sequestration” of reduced Cys^{51} in the active-site pocket [29]. Our observation of Prdx1 dimer formation is an indirect but most likely an accurate measurement of Prdx1 activity as was previously shown [17]. Overall, the complex cellular mechanism involved in Prdx1 scavenging likely play a role on the severity of ROS experienced by the different cells.

It was suggested that ROS exposure must reach a certain threshold in order to significantly promote DNA damage that would lead to LOH [9]. It was shown that only the higher dosages of H_2O_2 treatment (300–600μM) led to a significant 2–6 fold increase in MR mediated LOH frequency while no increase in LOH frequency was observed with a 200μM H_2O_2 treatment [9]. Lower amounts of ROS in T cells compared to fibroblasts and an absence of an effect with *Mlh1* down-regulation may explain why there was no significant increase in LOH frequency in *Prdx1*$^{-/-}$ T cells. The cell-type specific effect of a decrease in *Mlh1* expression in the absence of Prdx1 illustrates the complexity of mechanisms governing tumorigenesis in different tissues.

A possible mechanism underlying lymphoma formation in Prdx1 deficient mice could be de-regulation of c-Myc transcriptional regulation. The Prdx1 protein binds to the MBII region of the c-Myc protein [7], a region important for the transcriptional regulation of genes critical in the promotion of the cellular transformation (cell growth/proliferation and cell-cycle regulation) that is a key step in lymphomagenesis [30].

Our study indicated that increased *in vivo* ROS amounts may promote mutations in a cell type specific manner. This differential effect could be caused by differences in antioxidant defense and the relative robustness of the DNA repair machinery. Future studies would involve elucidating these differences through gene expression, protein interaction and enzyme activity assays in both fibroblasts and T cells with and without treatment of an exogenous stressor. Overall, our results suggest that the mechanism underlying the increased tumor predisposition in Prdx1-deficient mice may vary depending on tissue type.

Acknowledgments

We would like to thank Jennifer Schulte for performing the Prdx1 western blot analyses. This work was supported by grants from the National Institutes of Health [grant numbers ES011633, P30ES05022].

References

1. Yoshizumi M, Tsuchiya K, Tamaki T. Signal transduction of reactive oxygen species and mitogen-activated protein kinases in cardiovascular disease. J. Med. Inv. 2001; 48:11–24.
2. Claiborne A, Yeh JI, Mallett TC, Luba J, Crane EJ, Charrier V, Parsonage D. Protein-sulfenic acids: diverse roles for an unlikely player in enzyme catalysis and redox regulation. Biochem. 1999; 38:15407–15416. [PubMed: 10569923]
3. Neumann CA, Cao J, Manevich Y. Peroxiredoxin 1 and its role in cell signaling. Cell Cycle. 2009; 8:4072–4078. [PubMed: 19923889]
4. Cadet J, Berger M, Douki T, Ravanat JL. Oxidative damage to DNA: formation, measurement, and biological significance. Rev. Phys. Biochem. Pharm. 1997; 131:1–87.
5. Díaz-Llera S, Podlutsky A, Osterholm AM, Hou SM, Lambert B. Hydrogen peroxide induced mutations at the HPRT locus in primary human T-lymphocytes. Mut. Res. 2000; 469:51–61. [PubMed: 10946242]
6. Neumann CA, Krause DS, Carman CV, Das S, Dubey DP, Abraham JL, Bronson RT, Fujiwara Y, Orkin SH, Van Etten RA. Essential role for the peroxiredoxin Prdx1 in erythrocyte antioxidant defence and tumour suppression. Nature. 2003; 424:561–565. [PubMed: 12891360]
7. Egler RA, Fernandes E, Rothermund K, Sereika S, de Souza-Pinto N, Jaruga P, Dizdaroglu M, Prochownik EV. Regulation of reactive oxygen species, DNA damage, and c-Myc function by peroxiredoxin 1. Oncogene. 2005; 24:8038–8050. [PubMed: 16170382]
8. Turker MS, Gage BM, Rose JA, Elroy D, Ponomareva ON, Stambrook PJ, Tischfield JA. A novel signature mutation for oxidative damage resembles a mutational pattern found commonly in human cancers. Cancer Res. 1999; 59:1837–1839. [PubMed: 10213488]
9. Turner DR, Dreimanis M, Holt D, Firgaira FA, Morley AA. Mitotic recombination is an important mutational event following oxidative damage. Mut. Res. 2003; 522:21–26. [PubMed: 12517408]
10. Knudson AG. Mutation and cancer: statistical study of retinoblastoma. Proc. Natl. Acad. Sci. U.S.A. 1971; 68:820–823. [PubMed: 5279523]
11. Shao C, Deng L, Henegariu O, Liang L, Raikwar N, Sahota A, Stambrook PJ, Tischfield JA. Mitotic recombination produces the majority of recessive fibroblast variants in heterozygous mice. Proc. Natl. Acad. Sci. U.S.A. 1999; 96:9230–9235. [PubMed: 10430925]
12. Shao C, Deng L, Chen Y, Kucherlapati R, Stambrook PJ, Tischfield JA. Mlh1 mediates tissue-specific regulation of mitotic recombination. Oncogene. 2004; 23:9017–9024. [PubMed: 15480418]
13. Shao C, Deng L, Henegariu O, Liang L, Stambrook PJ, Tischfield JA. Chromosome instability contributes to loss of heterozygosity in mice lacking p53. Proc. Natl. Acad. Sci. U.S.A. 2000; 97:7405–7410. [PubMed: 10861008]
14. Meng Q, Skopek TR, Walker DM, Hurley-Leslie S, Chen T, Zimmer DM, Walker VE. Culture and propagation of Hprt mutant T-lymphocytes isolated from mouse spleen. Env. Mol. Mut. 1998; 32:236–243.
15. Yuan L, Inoue S, Saito Y, Nakajima O. An evaluation of the effects of cytokines on intracellular oxidative production in normal neutrophils by flow cytometry. Exp. Cell. Res. 1993; 209:375–381. [PubMed: 8262156]
16. Huo YY, Li G, Duan RF, Gou Q, Fu CL, Hu YC, Song BQ, Yang ZH, Wu DC, Zhou PK. PTEN deletion leads to deregulation of antioxidants and increased oxidative damage in mouse embryonic fibroblasts. Free Rad. Bio. Med. 2008; 44:1578–1591. [PubMed: 18275859]
17. Cao J, Schulte J, Knight A, Leslie NR, Zagozdzon A, Bronson R, Manevich Y, Beeson C, Neumann CA. Prdx1 inhibits tumorigenesis via regulating PTEN/AKT activity. EMBO J. 2009; 28:1505–1517. [PubMed: 19369943]

18. Shen WH, Balajee AS, Wang J, Wu H, Eng C, Pandolfi PP, Yin Y. Essential role for nuclear PTEN in maintaining chromosomal integrity. Cell. 2007; 128:157–170. [PubMed: 17218262]
19. Frankenberg-Schwager M, Becker M, Garg I, Pralle E, Wolf H, Frankenberg D. The role of non-homologous DNA end joining, conservative homologous recombination, and single-strand annealing in the cell cycle-dependent repair of DNA double-strand breaks induced by H_2O_2 in mammalian cells. Rad. Res. 2008; 170:784–793.
20. Harfe BD, Jinks-Robertson S. DNA mismatch repair and genetic instability. Ann. Rev. Gen. 2000; 34:359–399.
21. Jiricny J. The multifaceted mismatch-repair system. Nat. Rev. Mol. Cell. Bio. 2006; 7:335–346. [PubMed: 16612326]
22. Herman JG, Umar A, Polyak K, Graff JR, Ahuja N, Issa JP, Markowitz S, Willson JK, Hamilton SR, Kinzler KW, Kane MF, Kolodner RD, Vogelstein B, Kunkel TA, Baylin SB. Incidence and functional consequences of hMLH1 promoter hypermethylation in colorectal carcinoma. Proc. Natl. Acad. Sci. U.S.A. 1998; 95:6870–6875. [PubMed: 9618505]
23. Kane MF, Loda M, Gaida GM, Lipman J, Mishra R, Goldman H, Jessup JM, Kolodner R. Methylation of the hMLH1 promoter correlates with lack of expression of hMLH1 in sporadic colon tumors and mismatch repair-defective human tumor cell lines. Cancer Res. 1997; 57:808–811. [PubMed: 9041175]
24. Brenner C, Deplus R, Didelot C, Loriot A, Viré E, De Smet C, Gutierrez A, Danovi D, Bernard D, Boon T, Pelicci PG, Amati B, Kouzarides T, de Launoit Y, Di Croce L, Fuks F. Myc represses transcription through recruitment of DNA methyltransferase corepressor. EMBO J. 2005; 24:336–346. [PubMed: 15616584]
25. Gartel AL. A new mode of transcriptional repression by c-myc: methylation. Oncogene. 2006; 25:1989–1990. [PubMed: 16170342]
26. Felsher DW, Bishop JM. Transient excess of MYC activity can elicit genomic instability and tumorigenesis. Proc. Natl. Acad. Sci. U.S.A. 1999; 96:3940–3944. [PubMed: 10097142]
27. Jeong W, Park SJ, Chang TS, Lee DY, Rhee SG. Molecular mechanism of the reduction of cysteine sulfinic acid of peroxiredoxin to cysteine by mammalian sulfiredoxin. J. Bio. Chem. 2006; 277:14400–14407. [PubMed: 16565085]
28. Wood ZA, Schröder E, Robin Harris J, Poole LB. Structure, mechanism and regulation of peroxiredoxins. Trends Bio. Sci. 2003; 28:32–40.
29. Yang KS, Kang SW, Woo HA, Hwang SC, Chae HZ, Kim K, Rhee SG. Inactivation of human peroxiredoxin I during catalysis as the result of the oxidation of the catalytic site cysteine to cysteine-sulfinic acid. J Bio. Chem. 2002; 277:38029–38036. [PubMed: 12161445]
30. Marinkovic D, Marinkovic T, Kokai E, Barth T, Möller P, Wirth T. Identification of novel Myc target genes with a potential role in lymphomagenesis. Nuc. Acids Res. 2004; 32:5368–5378.

Highlights

- Significant elevation in ROS levels in *Prdx1*$^{-/-}$ T cells and ear fibroblasts
- Reduced Prdx1 peroxidase activity in fibroblasts compared to T cells
- Significant elevation in LOH mutant frequency only in Prdx1 deficient fibroblasts
- Significant reduction in Mlh1 expression in *Prdx1*$^{-/-}$ fibroblasts

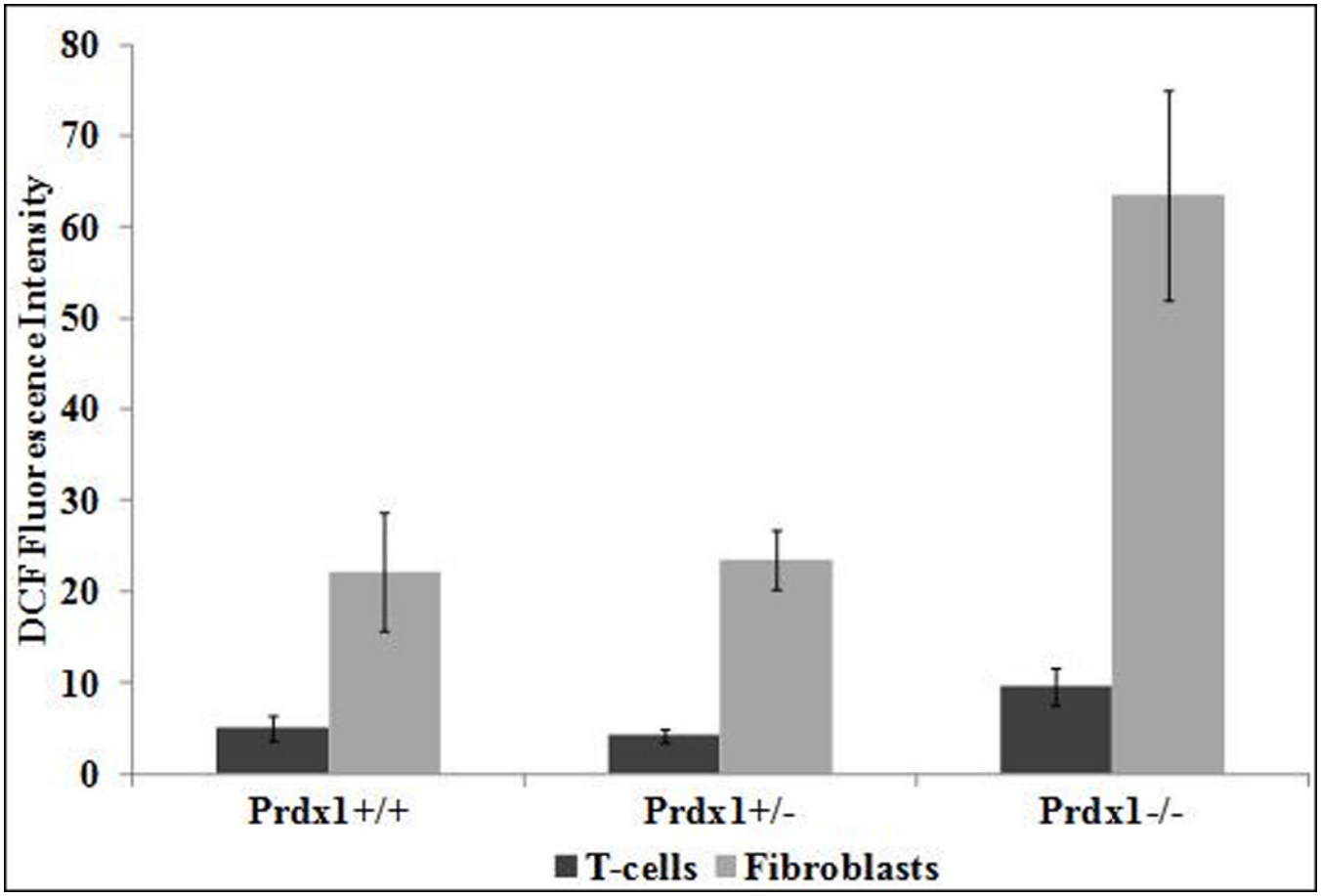

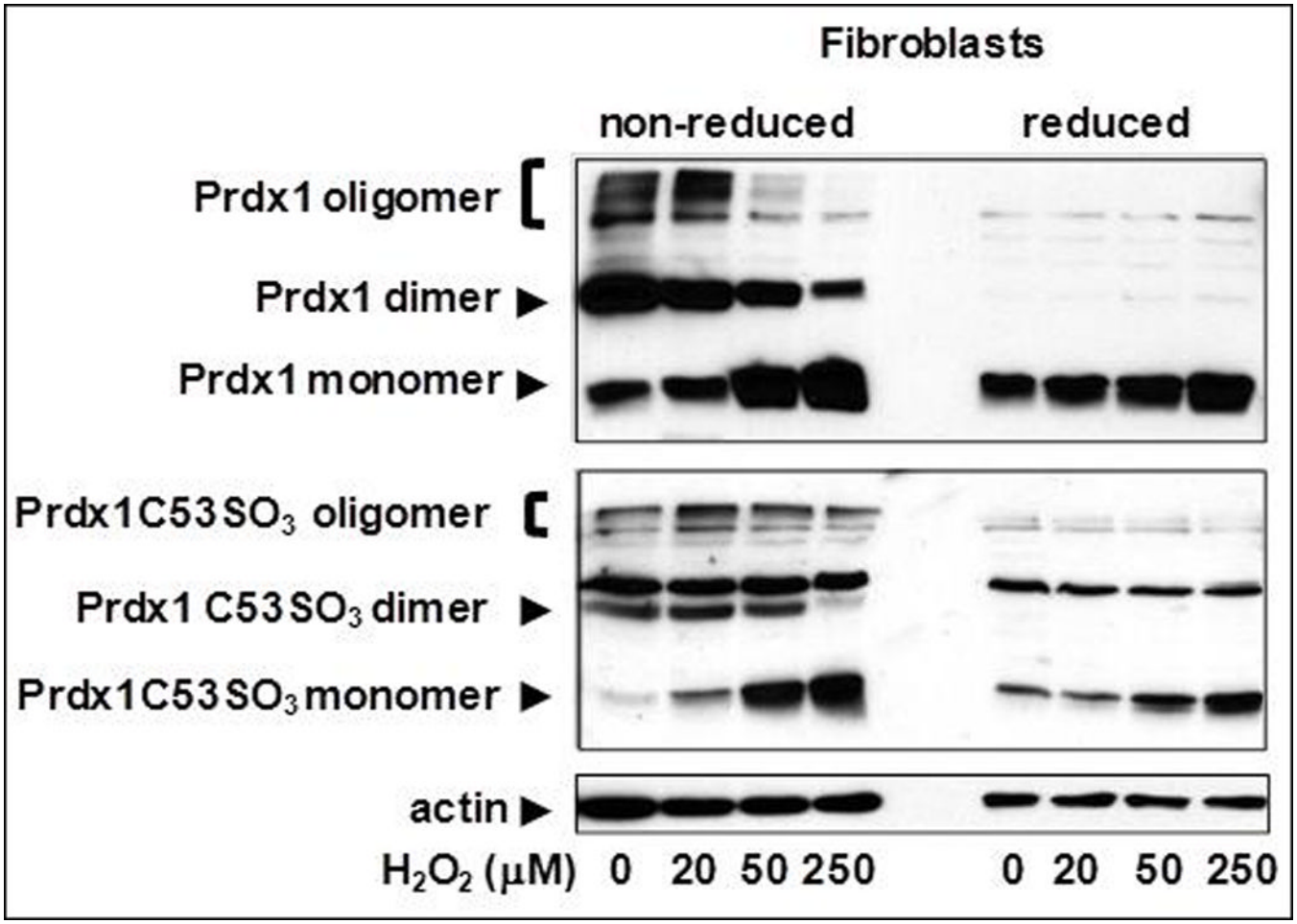

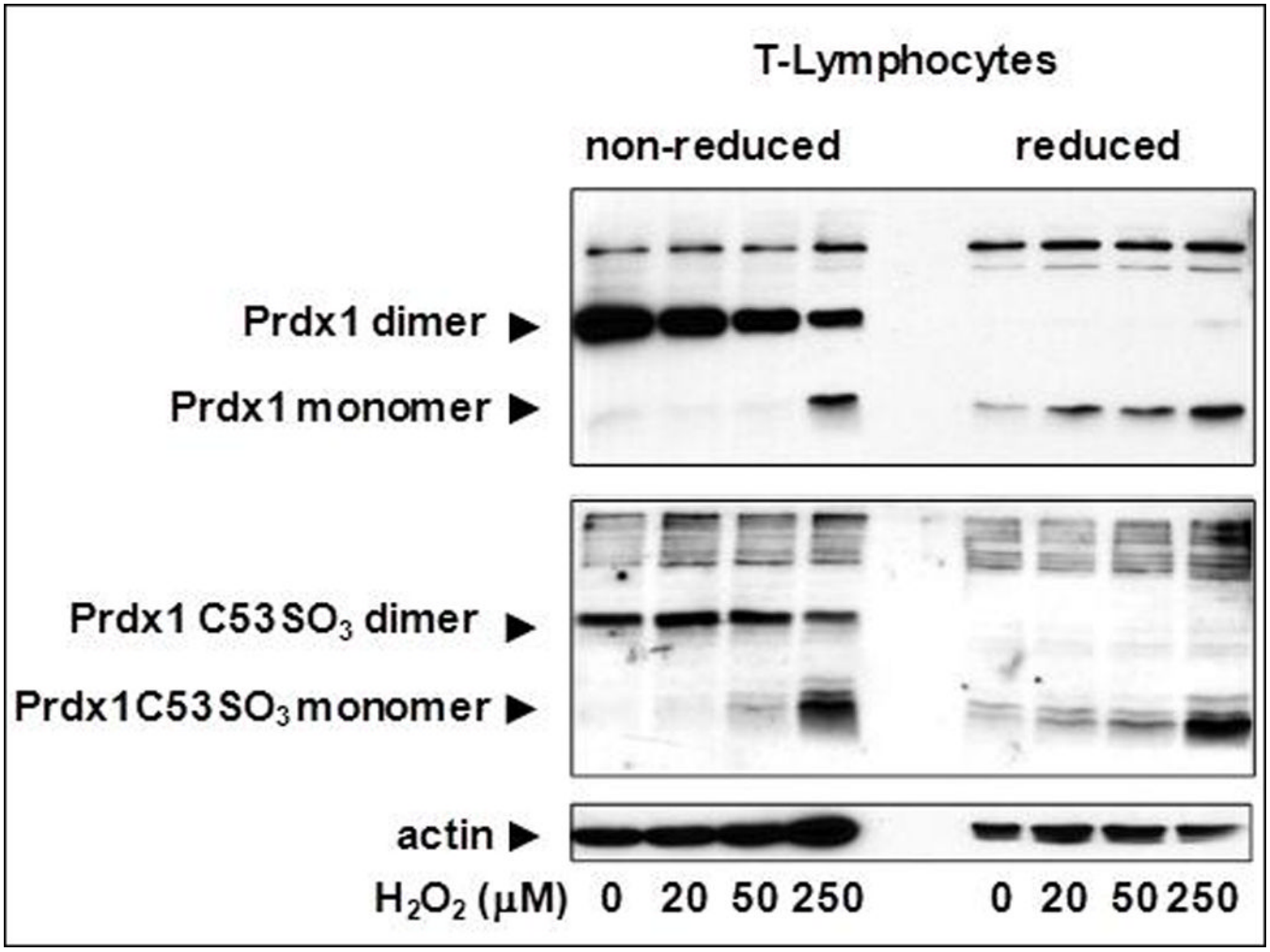

Fig. 1.

(A) DCF fluorescence intensity measured by flow cytometry in T cells and fibroblasts isolated from *Prdx1*$^{+/+}$, *Prdx1*$^{+/-}$ and *Prdx1*$^{-/-}$ mice. **(B)** and **(C)** Immunoblots of non-reduced and reduced (with beta-mercaptoethanol) protein lysates from H_2O_2 treated *Prdx1*$^{+/+}$ primary ear fibroblasts splenic T cells, respectively, prepared as discussed under Materials and Methods. Normal Prdx1 (top panels) and oxidized (Prdx1C53SO_3-bottom panels) protein expression. 30μg of protein was loaded per lane. * $p<0.05$

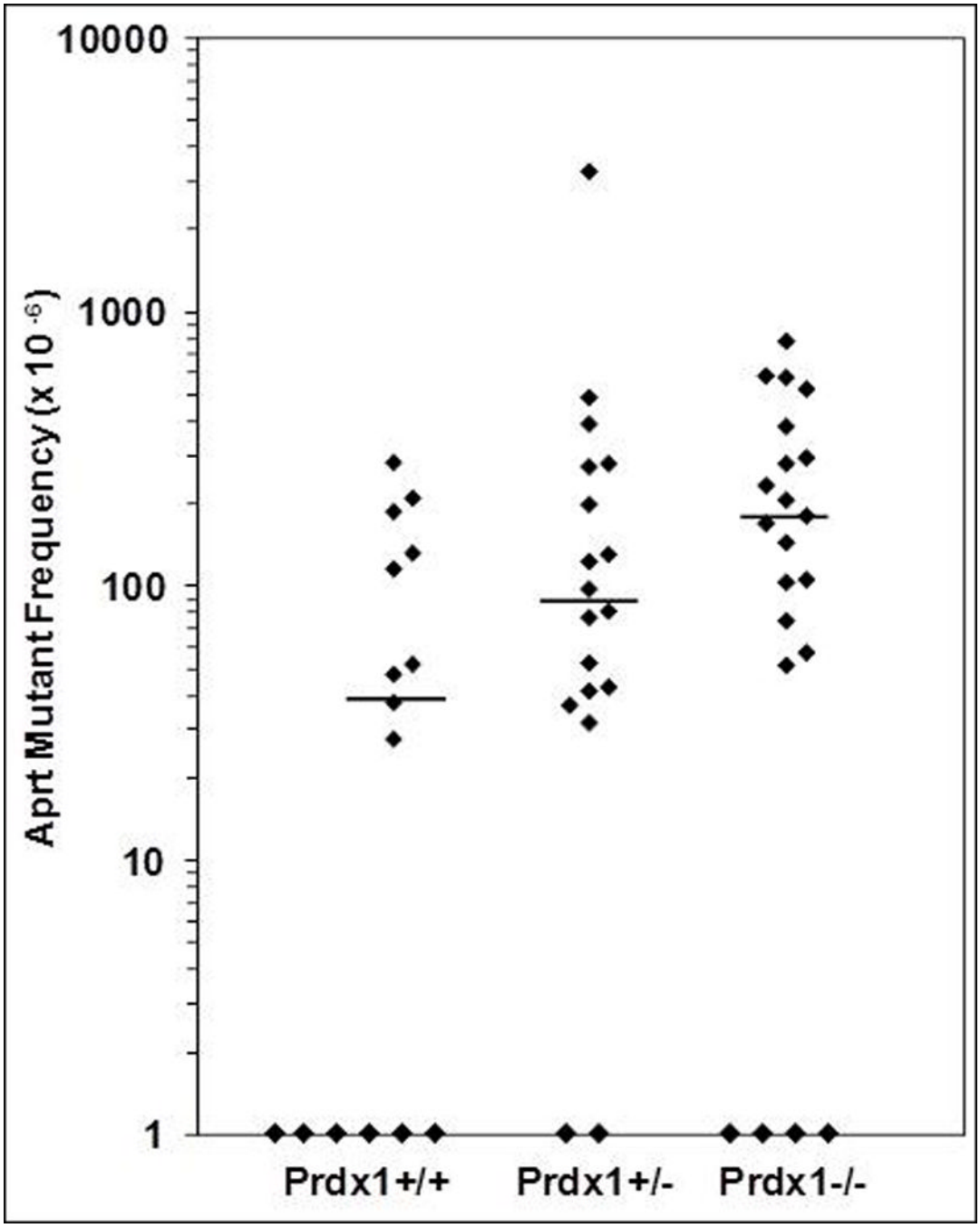

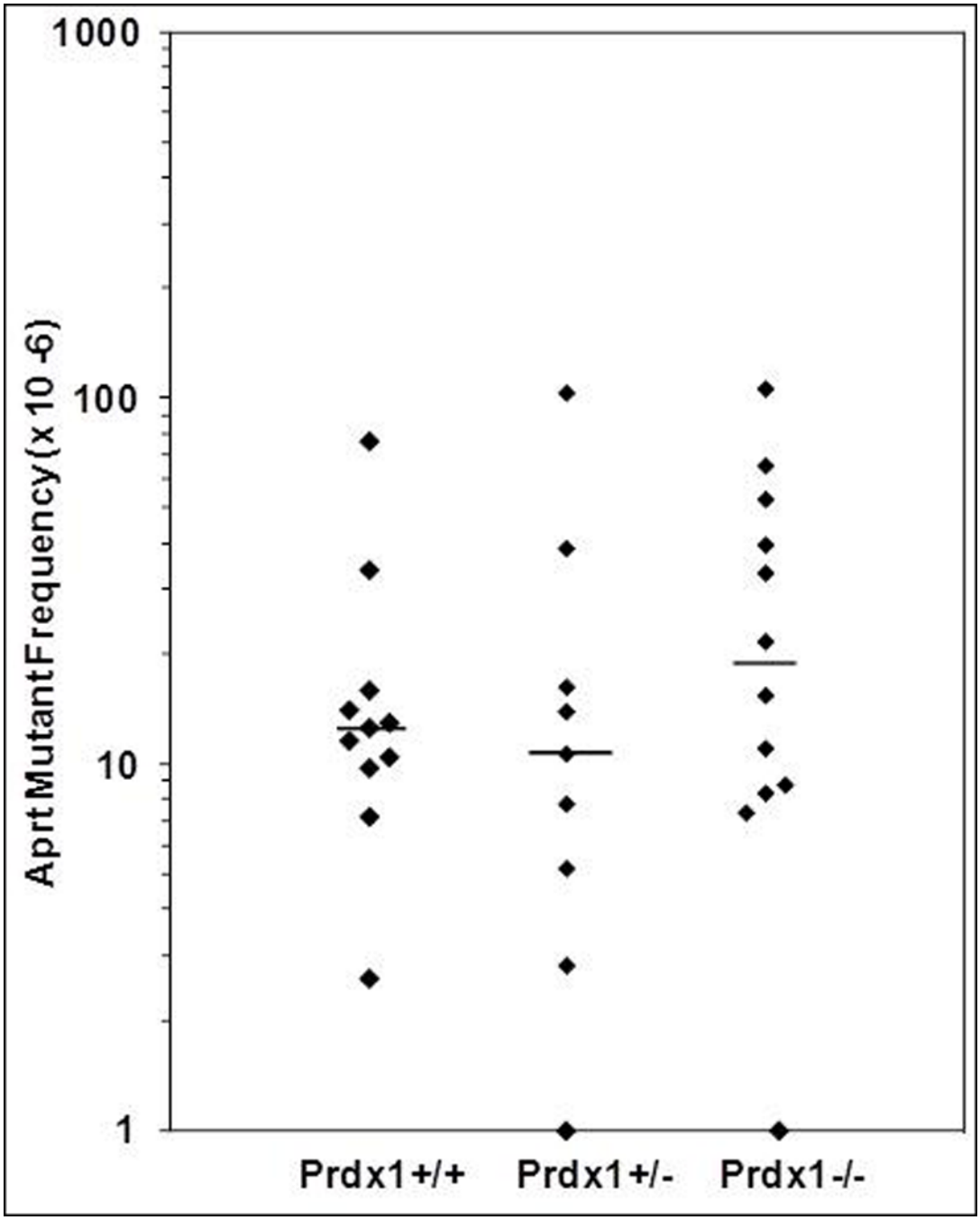

Fig. 2.

(A) Frequency of DAP^r fibroblasts in individual mouse ears where each point represents the frequency of DAP^r fibroblasts from one ear. **(B)** Frequency of DAP^r T cells from individual mouse spleens where each point represents the frequency of DAP^r T cells from one spleen. The bars indicate median frequencies. Points at the x-axis intersect represent fibroblast or T-cell cultures from which no DAP^r colonies were recovered.

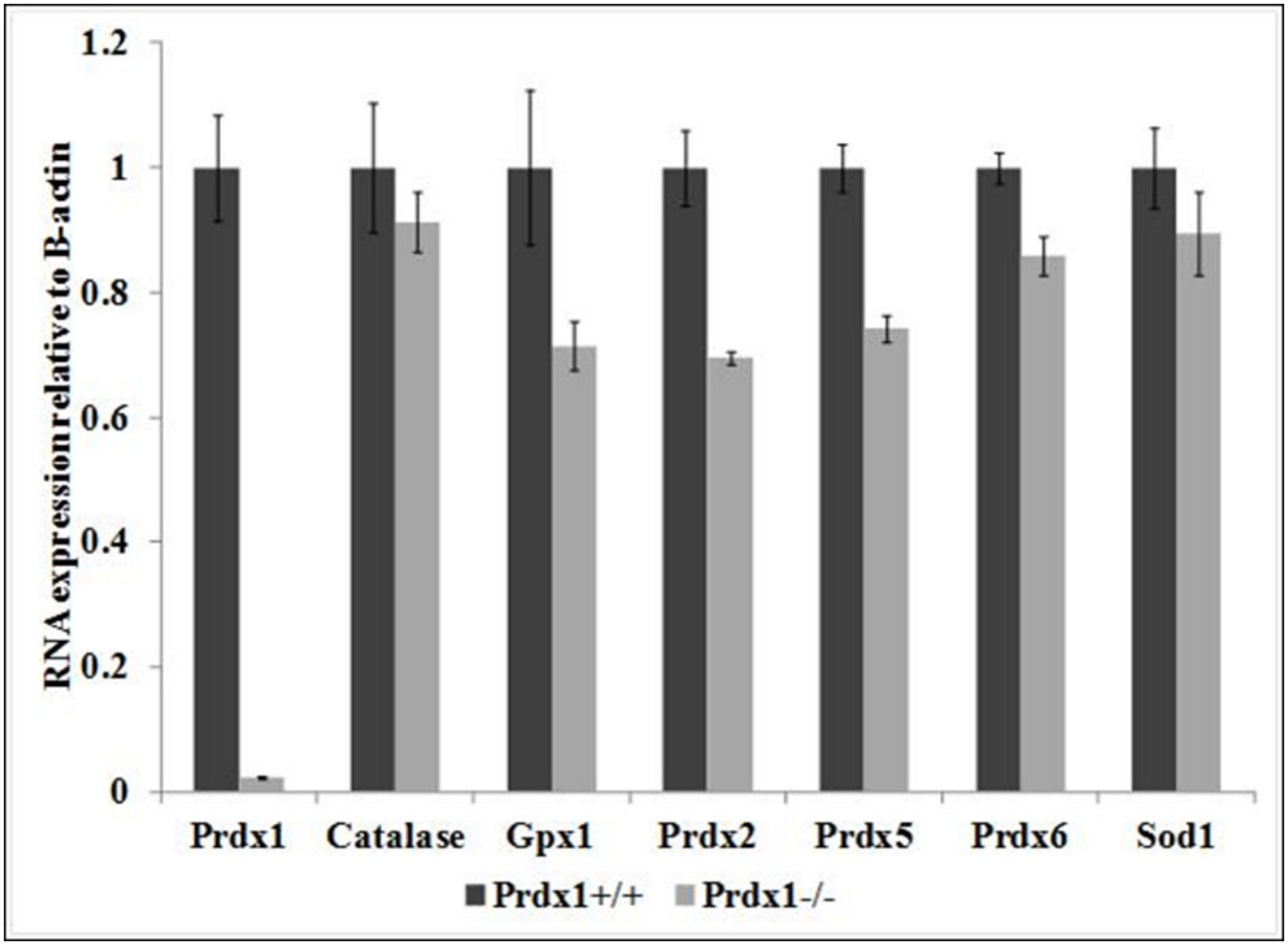

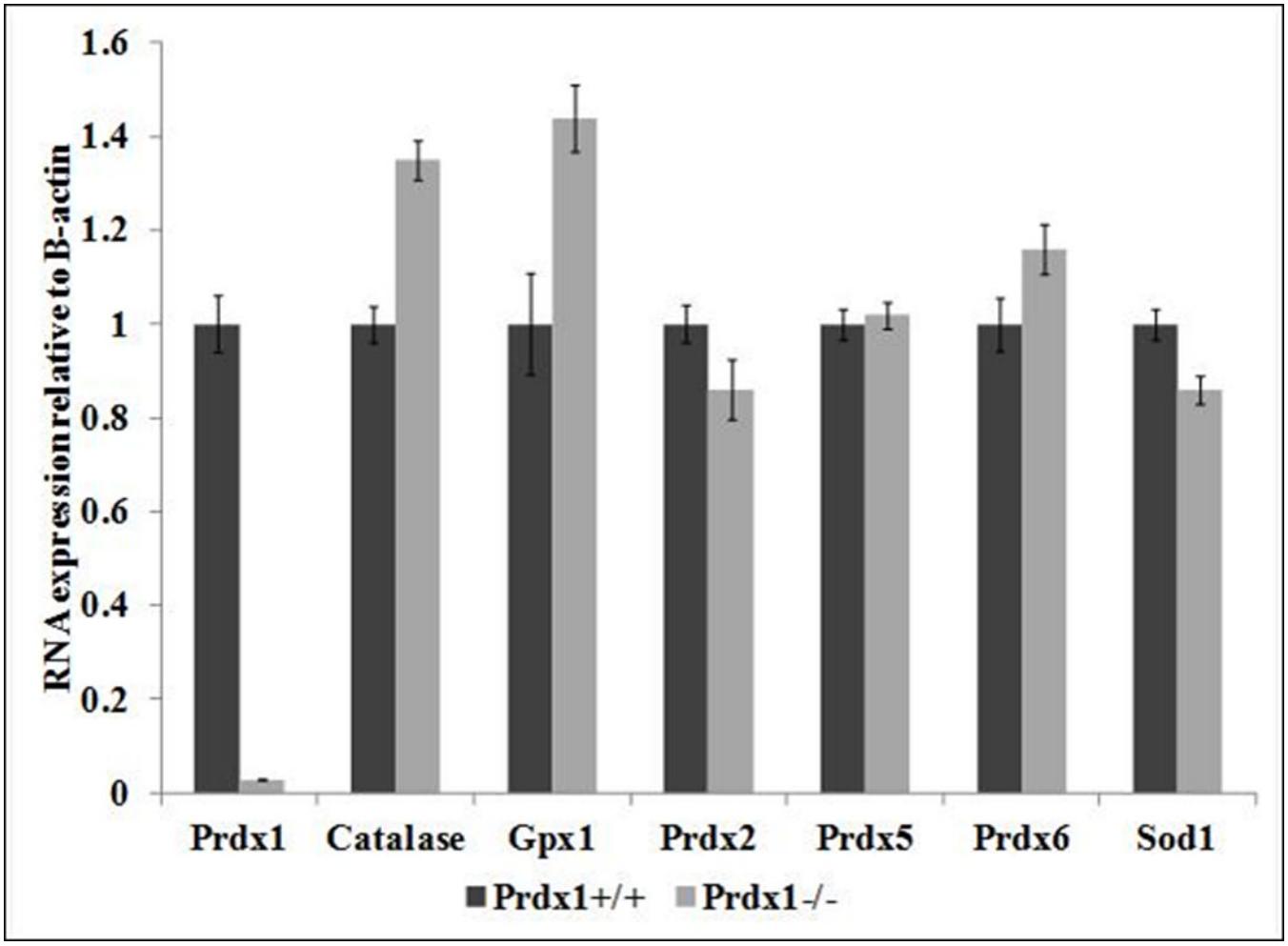

Fig. 3.

Relative mRNA expression of genes that encode antioxidant proteins in **(A)** T cells and in **(B)** primary fibroblasts derived from *Prdx1*$^{+/+}$ and *Prdx1*$^{-/-}$ mice. Expression of *Prdx1*$^{+/+}$ samples was normalized to 1.

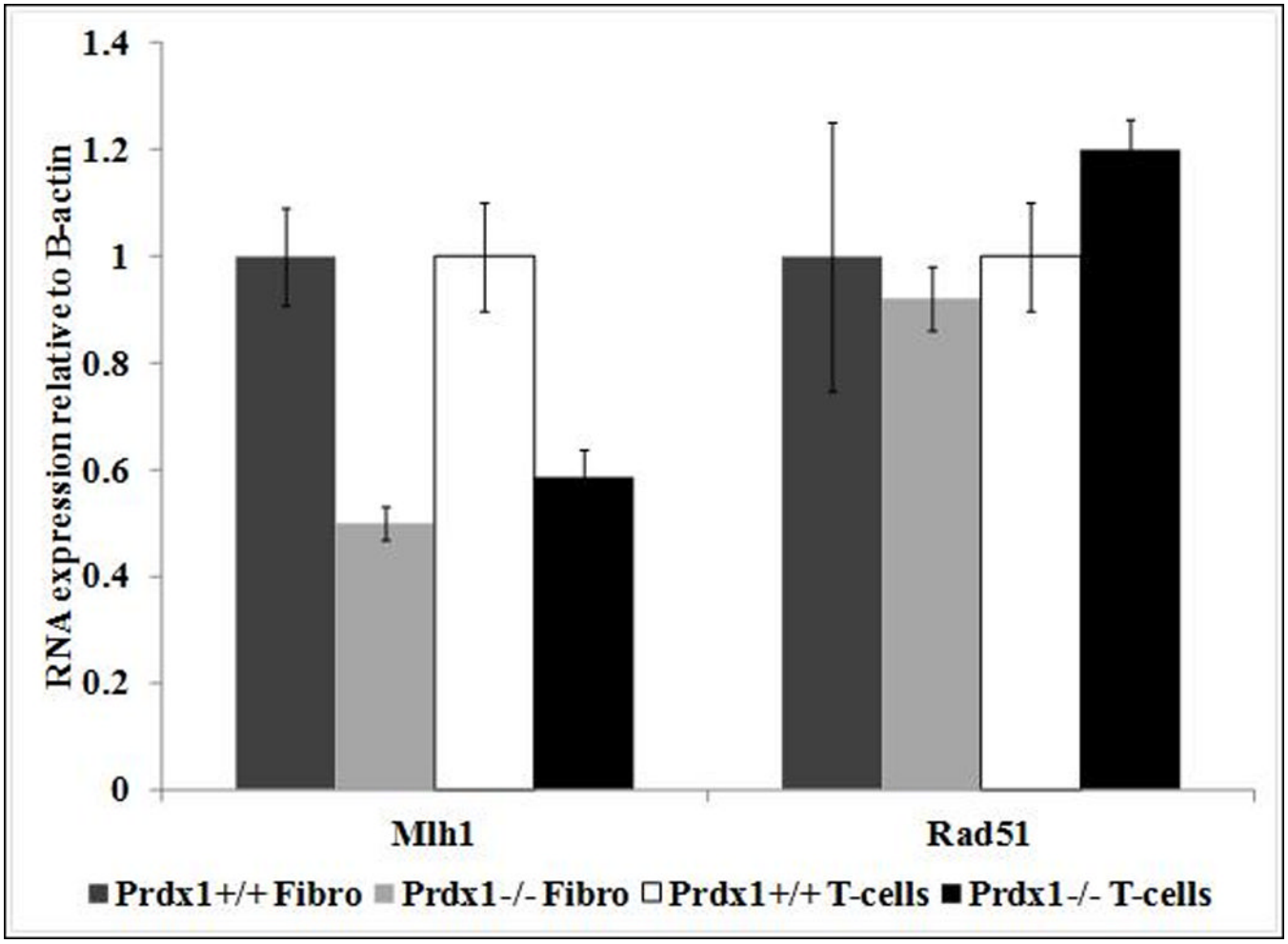

Fig. 4.

Relative mRNA expression of Mlh1 and Rad51 in *Prdx1*$^{+/+}$ and *Prdx1*$^{-/-}$ T cells and fibroblasts. *≥2-fold change and $p<0.05$. Expression of *Prdx1*$^{+/+}$ samples was normalized to 1.

Table 1

Sequence of RT primers of antioxidant genes used in qPCR experiments.

Gene	Accession No.	Forward Primer	Reverse Primer
B-actin	NM_007393.3	GACGGCCAGGTCATCACTATTG	AGTTTCATGGATGCCACAGGAT
Catalase	NM_009804.2	CCATCGCCAATGGCAATTAC	AGGCCAAACCTTGGTCAGATC
Gpx1	NM_008160.6	CCGCTTTCGTACCATCGACAT	CCAGTAATCACCAAGCCAATGC
Mlh1	NM_026810.2	CGGCCAATGCTATCAAAGAGA	CCAGTGCCATTGTCTTGGATC
Prdx1	NM_011034.4	AGTCCAGGCCTTCCAGTTCACT	GGCTTGATGGTATCACTGCCAG
Prdx2	NM_011563.5	AAGGACACCACTGGCATCGAT	CACACAATTACGGCGTGTTGAA
Prdx5	NM_012021.2	GTGTTTTGTTTGGAGTCCCTGG	AATAACGCTCAGACAGGCCAC
Prdx6	NM_007453.3	TTTGAGGCCAATACCACCATC	TGCCAAGTTCTGTGGTGCA
Rad51	NM_011234.4	AGCGTCAGCCATGATGGTAGAA	TTTGCCTGGCTGAAAGCTCTC
Sod1	NM_011434.1	AAGCATGGCGATGAAAGCG	ACAACACAACTGGTTCACCGC

Table 2

Cloning efficiency, mutant frequency and classification of clones derived from ear fibroblasts and T cells.

Cell Type	Genotype	No. of ears	Cloning efficiency % (mean±s.e.)	DAPr frequency ($\times 10^{-6}$)[a]	No. of DAPr colonies analyzed	% class I colonies	Class I frequency ($\times 10^{-6}$)[b]
Fibroblasts	*Prdx1*$^{+/+}$	15	1.29±0.07	37.9	16	75	28.4
	Prdx1$^{+/-}$	18	1.38±0.06	89.3*	31	74	66.3
	Prdx1$^{-/-}$	21	1.26±0.05	169*	53	79	134
Cell Type	*Genotype*	*No. of mice*	*Cloning efficiency % (mean ± s.e.)*	*DAPr frequency ($\times 10^{-6}$)[a]*	*No. of DAPr colonies analyzed*	*% class I colonies*	*Class I frequency ($\times 10^{-6}$)[b]*
T-cells	*Prdx1*$^{+/+}$	11	5.58 ± 1.17	11.6	33	82	9.5
	Prdx$^{1+/-}$	9	7.09 ± 1.42	10.7	34	79	8.5
	Prdx1$^{-/-}$	12	4.21 ± 1.01	18.4	37	89	16.4

[a] Median frequency.

[b] Calculated by multiplying DAP^r frequency and % class I.

* $p<0.05$, Mann Whitney U-test. s.e.- standard error.

Table 3

Mutational spectrum of class I clones in T-cells and fibroblasts.

Cell Type	Genotype	Mitotic recombination	Deletion or gene conversion	Chromosomal loss	Total no. of clones
Fibroblasts	*Prdx1*$^{+/+}$	12	0	0	12
	Prdx1$^{+/-}$	19	4	0	23
	Prdx1$^{-/-}$	35	1	6	42
T-cells	*Prdx1*$^{+/+}$	26	4	0	30
	Prdx1$^{+/-}$	24	3	0	27
	Prdx1$^{-/-}$	30	1	2	33